A SOM-based Gradient-Free Deep Learning Method with Convergence Analysis

Shaosheng Xu, Jinde Cao, Yichao Cao, Tong Wang, Wenhua Qian

***Abstract*—As gradient descent method in deep learning causes a series of questions, this paper proposes a novel gradient-free deep learning structure. By adding a new module into traditional Self-Organizing Map and introducing residual into the map, a Deep Valued Self-Organizing Map network is constructed. And analysis about the convergence performance of such a deep Valued Self-Organizing Map network is proved in this paper, which gives an inequality about the designed parameters with the dimension of inputs and the loss of prediction.**

***Index Terms*—Self-Organizing Map, deep learning, residual, gradient-free, convergence theory.**

I. Introduction

At present, the field of deep learning is developing rapidly, and layers of neural network go deeper and deeper. From the 3-5 layers' neural networks at the beginning to hundreds-layers' ones nowadays, the expression abilities of these networks have made a qualitative leap. However, the convergence method of them still mainly depends on the gradient-descent method [1]. With the development of optimization theory and the application of various new activation functions, the gradient-descent method based deep learning technologies has been improved gradually [2]–[4]. However, the problem of gradient explosion/vanishing still can not be solved completely. Moreover, the design of neural network hyper-parameters still lacks complete theory and it quite depends on the experience of researchers.

Our motivation is to design a method that can discard the gradient back propagation process in deep learning. There are two methods that attract our attention: Self-Organizing Map (SOM) and the residual idea. The former, also called Kohonen network [5], [6], is an typical unsupervised learning proposed by Professor Teuvo Kohonen of Helsinki University in Finland in 1981. Kohonen thinks that when such a model receives external inputs, it will be distinguished as different corresponding classes, which have different response characteristics to input modes and the process is finished automatically. And such characteristics are like those in the self-organization of mammal's brain. The advantage of SOM is that no gradient information is used in the training process, which ensures that the gradient explosion/vanishing problem never exists in this network. However, SOM can not integrate label information into training, which mean the supervised learning task cannot be achieved by this structure. And because of lacking deep structure, SOM's comprehensive ability on complex logy is weak.

A hierarchical self-organizing map(HSOM) has been proposed in 1992 [7]. Since the best matching neuron in SOM is closest to the input pattern and obtains the most effective information in the input, the authors made the best matching neuron feed back to the next self-organizing map as the input, which can save the network storage and reduce the computing cost. The effectiveness of HSOM has been proved in face recognition. While [8] focused on pattern recognition in time series and applies hierarchical self-organizing mapping (HSOM) to gesture recognition and achieves good results in 2008. After comparing traditional clustering methods, [9] proposed a general and online self-organizing map learning strategy, which is called self-organizing incremental neural network in 2006. This strategy introduces the insertion of the new node and the deletion of nodes with low probability density on self-organizing mapping network. Experiments show that this strategy can represent the topology of non-stationary data well in online learning and life-long learning tasks. And in order to reduce the number of network parameters and optimize the stability of structure, They put forward Enhanced Self-Organizing Incremental Neural Network (ESOINNN) [10] in the next year, which uses a single layer network instead of the two-layer structure of SOINN.

A great breakthrough was made in 2016, Deep Self-organizing Maps (DSOM) [11] was put forward by combining deep learning and self-organizing maps, which includes a self-organizing mapping layer composed of multiple self-organizing networks for extracting the information of different receptive field and a sampling layer is used to organizes the best matching neurons of each SOM, and constructs a fresh two-dimensional grid, whose function is to construct more global information at higher layers. The results show that DSOM performs well in extracting high-level abstract features. However, the excessive consumption of DSOM calculation limits its application. [12] put forward parallelizable deep self-organizing maps(PD-SOM) in 2017, the advantage of this network is that SOM of different sizes is used to learn features of different responses in the same layer, and PD-SOM originates from the unsupervised learning and does not use tags during training. Experiments show that the running time of PD-SOM is reduced by 18% compared with DSOM.

S. Xu is with the School of Automation, Southeast University, Nanjing 210096, China (e-mail: xushaosheng@seu.edu.cn).

J. Cao is with the School of Mathematics, and the Jiangsu Provincial Key Laboratory of Networked Collective Intelligence, Southeast University, Nanjing 210096, China (e-mail: jdcao@seu.edu.cn).

Y. Cao is with the School of Automation, Southeast University, Nanjing 210096, China (e-mail: caoyichao@seu.edu.cn).

T. Wang is is with the School of Mathematics,Southeast University, Nanjing 210096, China (e-mail: 220191489@seu.edu.cn).

W. Qian is with Department of Computer Science and Engineering, Yunnan University, Kunming 650000, China. (e-mail:whqian@ynu.edu.cn)

The ideal of the residual [13] is proposed by Microsoft Research Institute in 2015. The main contribution of the residual is the discovery of degradation and the invention of shortcut connection aiming at the degradation phenomenon, which greatly eliminates the problem of too deep neural network training difficulty.

This paper proposes a novel deep SOM network with supervised learning structure based on the original intention of DSOM and the basic idea of the residual. At the beginning of the design, we improved the original SOM and introduced a Lethe to each neuron, so that the network realizes the function of supervised learning. Then, we send the residual of the Lethe and the difference between the original input vectors and the best matching neuron as the new inputs into a next layer, so as to deepen the network layers. At the same time, in order to enhance the expression ability of the network, we add the "unfolding" operation in each layer, and analyze the relationship of its ability of approximating the nonlinear functions and the depth and the width of the network.

The main contributions of this paper are:

1. A novel structure of deep learning network, whose training process is gradient-free, is proposed.

2. The relationship between the loss and the structure of this network is proved.

The rest of this paper is organized as follows. The Valued SOM is designed and supervised learning rules for it is proposed and abstracted in section II. In section III, the ability of different layers to analyze the spatial structure is studied. With the batch normalization between each layer, the network structure of deep Valued SOM is realized. Besides, the different modes on training and testing are displayed respectively. In section IV, the "unfolding" operation is introduced and the upper bound of proposed network is proved. Furthermore, the relationship between the loss and the structure of this network is given in the inequality and in section V, the numerical experiment is conducted to verifies our convergence analysis.

II. Valued Self-Organizing Map with Supervised Learning Rules

The SOM, also called Kohonen network, is a widely used unsupervised learning model, which consists of input layer and competition/output layer. The output layer is a 1-dimensional or 2-dimensional grid array composed of several neurons [14]. As it fully connected, i.e., each input node is connected to all output ones, we let $W_{j,i}$, $i = 1, 2, ..., D$, $j = 1, 2, ..., N$ denote the weight between the neurons X_i in the input layer and the neurons C_j in the output layer. Suppose there are D neurons located in the layer of inputs, while N located in the layer of outputs. According to classic SOM model, the distance between a D-dimensional input vector $X = \langle X_1, X_2, ..., X_D\rangle \in \mathbb{R}^D$ and the weight vector $W_j = \langle W_{j,1}, W_{j,2}, ..., W_{j,N}\rangle \in \mathbb{R}^N$ of every neuron C_j is calculated to determine the best matching neuron (BMN), as

$$\mathfrak{m} = \arg \min_{j\in 1,2,...,N} \rho(X, W_j),$$

where $\rho(\cdot, \cdot)$ is some distance function. Next, a neighborhood of the $\mathfrak{m}$ s is determined, and the weight vector of the neurons in the neighborhood is adjusted according to the following formula.

$$W_j \leftarrow W_j + \alpha\eta_{j,\mathfrak{m}}(X - W_j),$$

where α is learning rate and $\eta_{j,\mathfrak{m}}$ is a measure between the neuron j and the neuron $j, \mathfrak{m}$, which is determined both by the topology of the output layer and the number of learning round. The adjustment process makes the weight vector of inner neuron close to the direction of input vector. With the learning, the learning rate may continue to decline, as well as the range of the neighborhood of best matching neuron. Gradually, the weight vectors of output neurons are separated from each other and each represents a cluster in the input space while the topology of the output layer is still reserved. It can be seen that SOM is an unsupervised process, whose output neuron C_j is composed of weight W_j.

Next, in order to introduce the supervision mechanism, we add a new variable L_j, $j = 1, 2, ..., N$, called Lethe, into each output neuron and denote each output neuron as (W_j, L_j). At the same time, the input changes from X into $(X; b)$, where b is the label or target. For classification task, it is recommended that $b \in [0, 1]^m$ in most cases, while $b \in \mathbb{R}^p$ is suggested for the fitting task. Here L_j is valued in the same space where the b is. The learning rule of it is designed as

$$\begin{cases} L_{\mathfrak{m}} \leftarrow L_{\mathfrak{m}} + \dfrac{b - L_{\mathfrak{m}}}{K_{\mathfrak{m}}}, \\ K_{\mathfrak{m}} \leftarrow K_{\mathfrak{m}} + 1, \end{cases}$$

where, $K_{\mathfrak{m}}$ is an positive integer who cumulates the updating times of the $\mathfrak{m}$ neuron.

Furthermore, the outputs of our designed module includes not only the Lethe but also the difference between the input vector and the weight of the $\mathfrak{m}$. Which means the item

$$X - W_{\mathfrak{m}}$$

is put into consideration in our research. Now we name our proposed module as Valued Self-Organizing Mapping(VSOM). For a batch of inputs $\{(X(\tau); b(\tau))|\tau = 1, 2, ..., \Gamma\}$, the surprised learning rule of it is listed as follows:

$$\begin{cases} \mathfrak{m}(\tau) = \arg \min\limits_{j\in 1,2,...,N} \rho(X(\tau), W_j), \\ W_j \leftarrow W_j + \alpha_\tau \eta_{\tau,j,\mathfrak{m}(\tau)}(X(\tau) - W_j), \\ L_{\mathfrak{m}(\tau)} \leftarrow L_{\mathfrak{m}(\tau)} + \dfrac{b(\tau) - L_{\mathfrak{m}(\tau)}}{K_{\mathfrak{m}(\tau)}}, \\ K_{\mathfrak{m}(\tau)} \leftarrow K_{\mathfrak{m}(\tau)} + 1, \\ \hat{X}_{(1)}(\tau) = X(\tau) - W_{\mathfrak{m}(\tau)}, \\ b_{(1)}(\tau) = b(\tau) - L_{\mathfrak{m}(\tau)}, \end{cases} \tag{1}$$

here the output of the Lethe is replaced by the residual $b(\tau) - L_{\mathfrak{m}(\tau)}$. The structure of VSOM is shown in Fig. 1.

Remark II.1. *As SOM can implement automatic clustering in unsupervised case, the cluster's label must maintain the the label's value, if the input vector with the same label automatically clustered. However, in general, every cluster may not have the same label, especially for the continuous function fitting task, there is no identical label nearly. Meanwhile, according to the update rules, it is easy to prove that any L_j will*

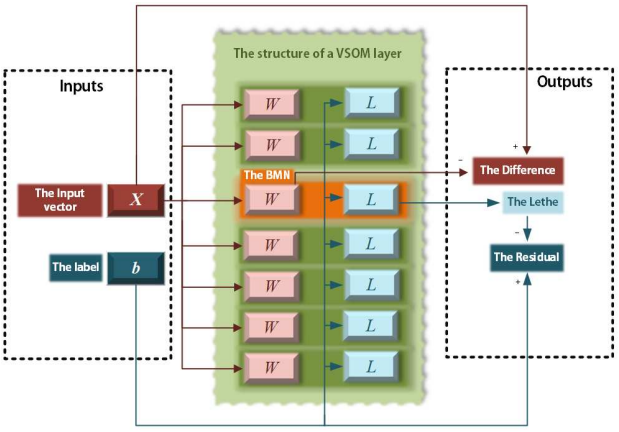

Fig. 1. The structure of VSOM.

converge to the weighted average value of its cluster's labels. Suppose $\{(X(\tau_k); b(\tau_k))|k = 1, 2, ..., \Gamma_0\}$ *are clustered into the some* $\mathfrak{m}$ *neuron* C_{j_0}*, the Lethe* $L_{j_0} = \frac{1}{\Gamma_0}\sum_{k=1}^{\Gamma_0} b(\tau_k) \to \frac{\Gamma}{\Gamma_0}\mathbb{E}[b(\tau)|\mathfrak{m}(\tau) = j_0]$*, where* $\mathbb{E}[\cdot|\cdot]$ *is conditional expectation [15]. It is obviously that the condition in the conditional expectation forms a subset of* $\Omega = \{1, 2, ..., \Gamma\}$*. According to the discussion, we define* $\mathfrak{F}$ *be a* σ*-algebra [16] generated by the subsets* $\{\tau|\mathfrak{m}(\tau) = j\}$*,* $j = 1, 2, ..., N$*, which is denoted by* $\mathfrak{F} = \sigma(\{\{\tau|\mathfrak{m}(\tau) = j\}|j = 1, 2, ..., N\})$ *and we can estimate the Lethe as*

$$L_{\mathfrak{m}(\tau)} = \mathbb{E}[b(\tau)|\mathfrak{F}],$$

if each $\Gamma_j = \|\{\tau|\mathfrak{m}(\tau) = j\}\|$ *is big enough, where the symbol* $\|\mathbb{A}\|$ *means the number of the members in set* $\mathbb{A}$*. In the same way we have done before, it is to get the following estimation*

$$W_{\mathfrak{m}(\tau)} = \mathbb{E}[X(\tau)|\mathfrak{F}].$$

For further discussing, we replace the notations $\mathfrak{F}$*,* X*,* b*,* W_j *and* $\mathfrak{m}$ *by* $\mathfrak{F}_1$*,* $X_{(0)}$*,* $b_{(0)}$*,* $W_j^{(0)}$ *and* $\mathfrak{m}_0$ *and the outputs of Eqs. (1), by getting rid of some trivial expressions, can be rewritten in a brief formation,*

$$\begin{cases} \mathfrak{F}_1 = \sigma(\{\{\tau|\mathfrak{m}_0(\tau) = j\}|j = 1, 2, ..., N\}), \\ \hat{X}_{(1)} = X_{(0)} - \mathbb{E}[X_{(0)}|\mathfrak{F}_1], \\ b_{(1)} = b_{(0)} - \mathbb{E}[b_{(0)}|\mathfrak{F}_1], \end{cases} \tag{2}$$

and the updating details are

$$\begin{cases} \mathfrak{m}_0(\tau) = \arg\min_{j\in 1,2,...,N} \rho(X_{(0)}(\tau), W_j^{(0)}), \\ W_j^{(0)} \leftarrow W_j^{(0)} + \alpha_\tau \eta_{\tau,j,\mathfrak{m}_0(\tau)}(X_{(0)}(\tau) - W_j^{(0)}), \\ L^0_{\mathfrak{m}_{(0)}(\tau)} \leftarrow L^{(0)}_{\mathfrak{m}_0(\tau)} + \dfrac{b_{(0)}(\tau) - L^{(0)}_{\mathfrak{m}_0(\tau)}}{K^{(0)}_{\mathfrak{m}_0(\tau)}}, \\ K^{(0)}_{\mathfrak{m}(\tau)} \leftarrow K^{(0)}_{\mathfrak{m}(\tau)} + 1, \end{cases}$$

and

$$\mathfrak{F}_1 = \sigma(\{\{\tau|\mathfrak{m}_0(\tau) = j\}|j = 1, 2, ..., N\}). \tag{3}$$

III. The Structure of Deep VSOM Network

As gradient-based methods are usually used in the optimizer of the deep learning, the gradient vanishing or explosion always confused many researchers. Although there are some way trying to avoid gradient vanishing or explosion, which actually partly solved such a confusing problem, the ghostly gradient vanishing or explosion still appears by surprise [17]–[19]. Nevertheless, the task of hyper parameters' adjustment in deep learning demands a lot of work. As many researchers make a lot of effort on these problems, this paper tries to give an answer in another way. That is, instead of solving the gradient vanishing or explosion problem, we just abandoned the gradient when we make our proposed network go deep. Now, we consider the VSOM module proposed in the former section as a layer. The inputs of the layer are $\{(X_{(0)}(\tau); b_{(0)}(\tau)), \tau = 1, 2, ..., \Gamma\}$ and the outputs are $\{(\hat{X}_{(1)}(\tau); b_{(1)}(\tau)), \tau = 1, 2, ..., \Gamma\}$. A natural way to deep the structure is to succeed the outputs of this layer and send them into an new layer. While, there are two questions need to answer in advance.

First, $b_{(1)}$ is the residual between the original inputs target and the conditional expectation which is estimated by the Lethe in the layer. No matter what kind of the problem there is, fitting or classification, $b_{(1)}(\tau)$ can be embedded in a D-dimensional field. Continuous or not, it has a zero conditional expectation on $\mathfrak{F}_1$ and can be obtained in the training process only. During testing or working after training, the Lethe $L^0_{\mathfrak{m}_{(0)}(\tau)}$, or say estimation of conditional expectation of the label in training set, can be observed. Fig. 2 illustrates the different working modes on training and testing respectively.

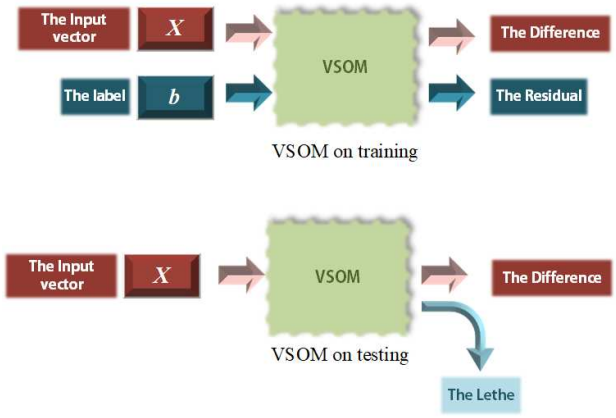

Fig. 2. Different modes of VSOM runs on training and testing respectively.

Second, The intuitive meaning of $\hat{X}_{(1)}$ is the division and superposition of the domain space. Suppose $W^{(0)}_{\mathfrak{m}_0}$ are the cluster centers, then $\hat{X}_{(1)}(\tau)$ is the difference vector from the vector of the nearest cluster center $W^{(0)}_{\mathfrak{m}_0}(\tau)$ to the vectors of the input $X_{(0)}(\tau)$, which is the difference vector from $W^{(0)}_{\mathfrak{m}_0}(\tau)$ to $X_{(0)}(\tau)$. If $\{X_{(0)}(\tau)|\tau = 1, 2, ..., \Gamma\}$ are uniformly distributed in the domain space, the difference vectors are also uniform. According to the definition, each cluster center is set to be 0 in $\hat{X}_{(1)}$, that is to say, all clusters are superimposed

with the center as the coincidence point. Mathematically, this process can be summarized as

$$\hat{X}_{(1)}(\tau) = \sum_{j=1}^{N} \hat{X}_{(1)}(\tau)\delta(\mathfrak{m}(\tau), j),$$

where $\delta(i,j) = 1$, if and only if $i = j$, else $\delta(i,j) = 0$. For convenance, we use the Norm-1 distance, which means $\rho(x,y) = \|x-y\|_1$, and display the division and superposition process intuitively in Fig. 3(a). It can be seen that the output

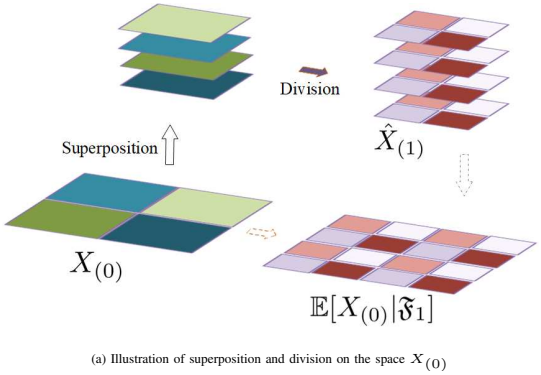

(a) Illustration of superposition and division on the space $X_{(0)}$

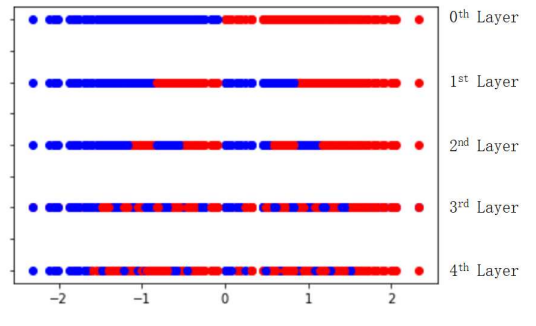

(b) Decomposition of a multi-layer VSOM on one-dimensional space with batch normalization.

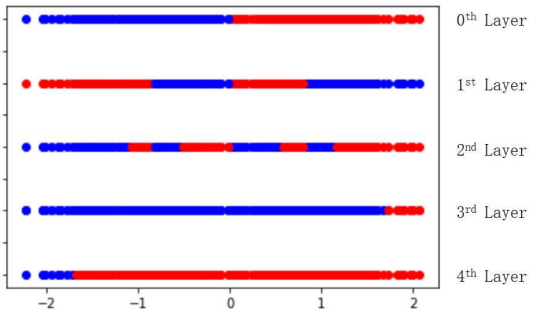

(c) Decomposition of a multi-layer VSOM on one-dimensional space without batch normalization.

Fig. 3. The illustration of superposition and division and the display of decomposition, (a) is a diagram of the superposition and division under the assumption that the clustering centers are uniformly distributed theoretically. (b) is the display of real effect in a multi-layer VSOM of two neurons in each layer with batch normalization. (c) is the display of real effect in a multi-layer VSOM of two neurons in each layer without batch normalization.

vectors are in a smaller size than the input ones. If we put them directly into a next layer, it may cause the space vanishing little by little when layers goes deep and finally fail to form clusters in deep layer. For that reason, it is necessary to introduce a batch normalization layer [20] succeed the outputs of each layer. That is

$$X_{(1)} = \mathfrak{B}_1(\hat{X}_{(1)}),$$

where $\mathfrak{B}_1$ is a affine mapping from $\mathbb{R}^D$ to $\mathbb{R}^D$. And for some i, it has the forms as bellow,

$$\mathfrak{B}_i(x) = \mathcal{K}_i \odot (x - \mathcal{B}_i),$$

where $\mathcal{K}_i$ and $\mathcal{B}_i$ have the same dimensions with x, and $\odot$ means Hardamard product. Both $\mathcal{K}_i$ and $\mathcal{B}_i$ must be irrelative with the sample's number in a batch. The difference of decomposition abilities of one with batch normalization and one without batch normalization is illustrated in Fig. 3(b) and Fig. 3(c).

Now we construct a novel deep learning model named Deep VSOM(DVSOM) Network. Suppose there are $\mathfrak{n}$ layers in this Network, $(W^{(\mathfrak{l})}, \mathfrak{m}_\mathfrak{l}, L^{(\mathfrak{l})}, K^{(\mathfrak{l})}, \mathfrak{B}_\mathfrak{l})$ for $\mathfrak{l} = 0, 1, ..., \mathfrak{n}-1$ and for each $\mathfrak{l}$, $(W^{(\mathfrak{l})}, \mathfrak{m}_\mathfrak{l}, L^{(\mathfrak{l})}, K^{(\mathfrak{l})})$ is a single VSOM layer, where

$$\begin{cases} W^{(\mathfrak{l})} = (W_1^{(\mathfrak{l})}, W_2^{(\mathfrak{l})}, ..., W_N^{(\mathfrak{l})}), \\ L^{(\mathfrak{l})} = (L_1^{(\mathfrak{l})}, L_2^{(\mathfrak{l})}, ..., L_N^{(\mathfrak{l})}), \\ K^{(\mathfrak{l})} = (K_1^{(\mathfrak{l})}, K_2^{(\mathfrak{l})}, ..., K_N^{(\mathfrak{l})}). \end{cases}$$

Then for the training set $\{(X_{(0)}(\tau); b_{(0)}(\tau)), \tau = 1, 2, ..., \Gamma\}$, the training process of $\mathfrak{n}$-layers DVSOM Network is

$$\begin{cases} \mathfrak{m}_\mathfrak{l}(\tau) = \arg\min\limits_{j\in 1,2,...,N} \rho(X_{(\mathfrak{l})}(\tau), W_j^{(\mathfrak{l})}), \\ W_j^{(\mathfrak{l})} \leftarrow W_j^{(\mathfrak{l})} + \alpha_\tau \eta_{\tau,j,\mathfrak{m}_\mathfrak{l}(\tau)}(X_{(\mathfrak{l})}(\tau) - W_j^{(\mathfrak{l})}), \\ L^{\mathfrak{l}}_{\mathfrak{m}_{(\mathfrak{l})}(\tau)} \leftarrow L^{(\mathfrak{l})}_{\mathfrak{m}_\mathfrak{l}(\tau)} + \dfrac{b_{(\mathfrak{l})}(\tau) - L^{(\mathfrak{l})}_{\mathfrak{m}_\mathfrak{l}(\tau)}}{K^{(\mathfrak{l})}_{\mathfrak{m}_\mathfrak{l}(\tau)}}, \\ K^{(\mathfrak{l})}_{\mathfrak{m}(\tau)} \leftarrow K^{(\mathfrak{l})}_{\mathfrak{m}(\tau)} + 1, \\ X_{(\mathfrak{l}+1)}(\tau) = \mathfrak{B}_\mathfrak{l}(X_{(\mathfrak{l})}(\tau) - W^{(\mathfrak{l})}_{\mathfrak{m}_\mathfrak{l}(\tau)}), \\ b_{(\mathfrak{l}+1)}(\tau) = b_{(\mathfrak{l})}(\tau) - L^{(\mathfrak{l})}_{\mathfrak{m}_\mathfrak{l}(\tau)}, \\ \tau \in \{1, 2, ..., \Gamma\}, \end{cases}$$

for each $\mathfrak{l} = 0, 1, ..., \mathfrak{n}-1$, the model is trained in order. And for the testing set $\{\tilde{X}_{(0)}(\tau), \tau = 1, 2, ..., \tilde{\Gamma}\}$, the testing process of this network is

$$\begin{cases} \mathfrak{m}_\mathfrak{l}(\tau) = \arg\min\limits_{j\in 1,2,...,N} \rho(\tilde{X}_{(\mathfrak{l})}(\tau), W_j^{(\mathfrak{l})}), \\ \tilde{X}_{(\mathfrak{l}+1)}(\tau) = \mathfrak{B}_\mathfrak{l}(\tilde{X}_{(\mathfrak{l})}(\tau) - W^{(\mathfrak{l})}_{\mathfrak{m}_\mathfrak{l}(\tau)}), \\ p_{(\mathfrak{l})}(\tau) = L^{(\mathfrak{l})}_{\mathfrak{m}_\mathfrak{l}(\tau)}, \\ \tau = 1, 2, ..., \tilde{\Gamma}, \\ \mathfrak{l} = 0, 1, ..., \mathfrak{n}-1, \end{cases}$$

and the final prediction of the label of sample $\tilde{X}_{(0)}(\tau)$ is

$$\mathfrak{p}(\tau) = \sum_{\mathfrak{l}=0}^{\mathfrak{n}-1} p_{(\mathfrak{l})}(\tau).$$

The structure of DVSOM with different modes are illustrated in Fig. 4.

Remark III.1. *As discussion in Remark II.1, the outputs of each layers can be rewritten as*

$$\begin{cases} \mathfrak{F}_{\mathfrak{l}+1} = \sigma(\{\{\tau|\mathfrak{m}_\mathfrak{l}(\tau) = j\}|j = 1, 2, ..., N\}), \\ X_{(\mathfrak{l}+1)}(\tau) = \mathfrak{B}_\mathfrak{l}(X_{(\mathfrak{l})}(\tau) - \mathbb{E}[X_{(\mathfrak{l})}|\mathfrak{F}_{\mathfrak{l}+1}]), \\ b_{(\mathfrak{l}+1)}(\tau) = b_{(\mathfrak{l})}(\tau) - \mathbb{E}[b_{(\mathfrak{l})}|\mathfrak{F}_{\mathfrak{l}+1}], \end{cases} \tag{4}$$

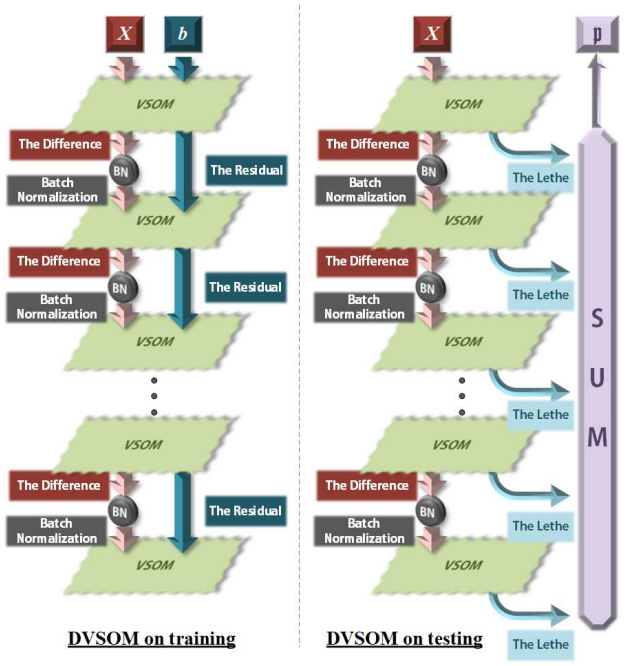

Fig. 4. The illustration of the structure of DVSOM and its different modes on training and testing respectively.

Remark III.2. *From the training process, it can be seen that* $b_{(0)}(\tau) = L^{(0)}_{\mathfrak{m}_0(\tau)} + b_{(1)}(\tau) = L^{(0)}_{\mathfrak{m}_0(\tau)} + L^{(1)}_{\mathfrak{m}_1(\tau)} + b_{(2)}(\tau) = \cdots = \sum_{\mathfrak{l}=0}^{\mathfrak{n}-1} L^{(\mathfrak{l})}_{\mathfrak{m}_\mathfrak{l}(\tau)} + b_{(\mathfrak{n})}(\tau)$. *It yields that, on the training set,*

$$b_{(0)}(\tau) = \mathfrak{p}(\tau) + b_{(\mathfrak{n})}(\tau).$$

It can be seen that $b_{(\mathfrak{n})}(\tau)$ is loss of the predict. From pervious the discussion in this paper, it yields

$$\mathbb{E}[b_{(0)} - \mathfrak{p}] = \mathbb{E}[b_{(\mathfrak{n})}] = \mathbb{E}[\mathbb{E}[b_{(\mathfrak{n})}|\mathfrak{F}_\mathfrak{n}]] = 0,$$

which means that the prediction has a bias of 0. Now it is expected that the variance $\mathbb{D}[b_{(\mathfrak{n})}] = \mathbb{E}[b^2_{(\mathfrak{n})}]$ is small enough or it declines as the number layers increases.

IV. Convergence Analysis

At the beginning of this section, we assume that the distribution of samples $\{X_{(0)}(\tau), \tau = 1, 2, ..., \Gamma\}$ in domain space is uniform and the number of them sufficient, so, after the training process proceeding, $\{X_{(\mathfrak{l})}(\tau), \tau = 1, 2, ..., \Gamma\}$ in each layer is also uniform distributed with sufficient number according to the analysis in the former section. For convenience, we assume that all neurons of an output layer form different cluster centers and the space of input vectors is bounded.

More strictly, let the samples be dense in domain space everywhere and the clustering is uniform. When every time the sample go through a VSOM layer, the samples will be cut into N parts. Because of the density of the samples, any neighborhood of any point of each part has intersection with other parts after superposition. In other words, after going through the next VSOM layer, each part will be divided into N parts again, so after $\mathfrak{n}$ VSOM layers, the sequence corresponding to the original sample space will be divided into $N^\mathfrak{n}$ parts with the same size.

Now let us deal with the residual equation in Eqs. (4), i.e.

$$b_{(\mathfrak{l}+1)}(\tau) = b_{(\mathfrak{l})}(\tau) - \mathbb{E}[b_{(\mathfrak{l})}|\mathfrak{F}_{\mathfrak{l}+1}].$$

By the analysis in Remark III.2, the variance of residuals of the $\mathfrak{l}$-layer is $\mathbb{E}[b^2_{(\mathfrak{l}+1)}]$. and according to Theorem IV.1, the following recurrence relation holds,

$$\mathbb{E}[b^2_{(\mathfrak{l}+1)}] = \mathbb{E}[b^2_{(\mathfrak{l})}] - \mathbb{E}[(\mathbb{E}[b_{(\mathfrak{l})}|\mathfrak{F}_{\mathfrak{l}+1}])^2]. \tag{5}$$

Theorem IV.1. *For stochastic variables* ξ, η *and a* σ*-algebra* $\mathfrak{F}$*, the following equation*

$$\mathbb{E}[\eta^2] = \mathbb{E}[\xi^2] - \mathbb{E}[(\mathbb{E}[\xi|\mathfrak{F}])^2] \tag{6}$$

holds, if they satisfy

$$\eta = \xi - \mathbb{E}[\xi|\mathfrak{F}].$$

Proof. Considering that $\mathbb{E}[\eta^2|\mathfrak{F}] = \mathbb{E}[\xi^2|\mathfrak{F}] - (\mathbb{E}[\xi|\mathfrak{F}])^2$, and according to the law of total expectation [21], the Eq. (6) holds. □

For all $\mathfrak{l} \in \{0, 1, ..., n-1\}$, if there is a non-negative φ, which satisfies that

$$\frac{\mathbb{E}[(\mathbb{E}[b_{(\mathfrak{l})}|\mathfrak{F}_{\mathfrak{l}+1}])^2]}{\mathbb{E}[b^2_{(\mathfrak{l})}]} \geq \varphi,$$

it can be seen that $\mathbb{E}[b^2_{(\mathfrak{n})}] \leq (1-\varphi)^\mathfrak{n}\mathbb{E}[b^2_{(0)}]$ according to Eq. (5).

According to Jensen's Inequality [22] and the law of total expectation, $\varphi \leq 1$ definitely. And $\varphi \geq 0$ is also obvious. Besides, a better estimation of φ is difficult indeed, as both of 0 and 1 can be reached really. It seems that φ depends on the specific situation.

For the linear function fitting task, $b(X) = kX$, where $X \in [-B, B]^D$ is a $(D \times 1)$-shape vector and k is a $(1 \times D)$-shape vector. For convenience, we assume the cluster centers of any VSOM layer are uniform distributed on an identical fastest descending line, and suppose each layer has $N = 2^m$ neurons. According to the method of calculus, $\frac{\mathbb{E}[(\mathbb{E}[b_{(\mathfrak{l})}|\mathfrak{F}_{\mathfrak{l}+1}])^2]}{\mathbb{E}[b^2_{(\mathfrak{l})}]} = \frac{N^2-1}{N^2}$, so the loss $\mathbb{E}[b^2_{(\mathfrak{n})}] = \mathbb{E}[b^2_{(0)}](\frac{1}{N^2})^\mathfrak{n}$. But in a D-dimensional space, the effective cluster centers' projection on a fastest descending line is approximately proportional to $\sqrt[D]{N}$ as the distribution of these centers is uniform as assumed before. So we finally estimate the **loss** $= \mathbb{E}[b^2_{(\mathfrak{n})}] = p_1(\frac{1}{N})^{p_0\frac{\mathfrak{n}}{D}}$, i.e.,

$$\log(\textbf{loss}) = p_0\frac{\mathfrak{n}}{D}\log(\frac{1}{N}) + \log p_1,$$

where p_0 and p_1 are both positive.

Remark IV.2. *It can be seen that the loss is an exponential function with the depth of network as the exponent. According to the mechanics of VSOM, if there is any bias in* $b(\cdot)$*, the bias will be filtered rapidly in the 0th layer of DVSOM, so the influence of bias can be ignored. And it is obvious that* $p_1 = p_1(k)$ *satisfies* $\|k\| \leq C_k \Rightarrow \exists C_p > 0, p_1 \leq C_p$.

For the same loss and number of neurons, the depth is proportional to the dimension of the domain space. It is

an ideal conclusion as we assume that the cluster centers are uniformly distributed in the domain space, while this assumption may be broken when the division times rise.

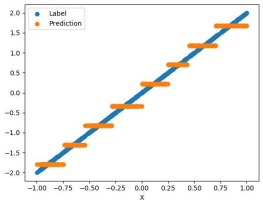

(a) 3-layer DVSOM's prediction of a linear function.

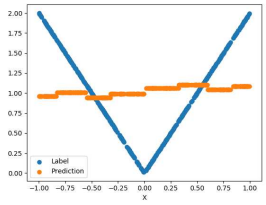

(b) 3-layer DVSOM's prediction of an absolution function.

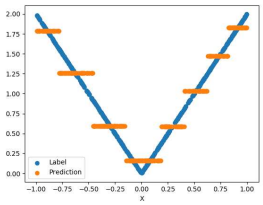

(c) 3-layer DVSOM's prediction of an absolution function with "unfolding" in each layer.

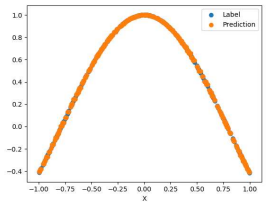

(d) 7-layer DVSOM's prediction of a cosine function with "unfolding" in each layer.

Fig. 5. The predictions of DVSOM whose each layer has two neurons. (a) and (b) are from the DVSOM without "unfolding", while (c) and (d) are from the DVSOM with "unfolding" in each layer

Another problem may arise when the condition expectation vanishes. Take the Eq. (5), when $\mathbb{E}[(\mathbb{E}[b_{(\mathfrak{l})}|\mathfrak{F}_{\mathfrak{l}+1}])^2]$ tends to 0, we get $\mathbb{E}[b^2_{(\mathfrak{l}+1)}] \to \mathbb{E}[b^2_{(\mathfrak{l})}]$. That problem happens on even functions with symmetric intervals when there is only two neurons in a layer, as seen in Fig. 5 (a) and (b). To avoid this problem, the main idea is to prevent $\mathbb{E}[b_{(\mathfrak{l})}|\mathfrak{F}_{\mathfrak{l}+1}]$ being 0 and this idea can be achieved by select a series of subsets of $\Omega = \{1, 2, ..., \Gamma\}$, for example $\Omega_1, \Omega_2, ..., \Omega_k$, which satisfy $\Omega_i \cap \Omega_j = \emptyset$ for all $i \neq j$ and $\bigcup_{i=1}^{\Gamma} \Omega_i = \Omega$, are not the elements of σ-Algebra $\mathfrak{F}_{\mathfrak{l}+1}$, so that $\mathbb{E}[\mathbb{I}_{\Omega_i} b_{(\mathfrak{l})}|\mathfrak{F}_{\mathfrak{l}+1}] \neq 0$. So the recurrence relation can be rewritten as,

$$\mathbb{I}_{\Omega_i} b_{(\mathfrak{l}+1)}(\tau) = \mathbb{I}_{\Omega_i} b_{(\mathfrak{l})}(\tau) - \mathbb{E}[\mathbb{I}_{\Omega_i} b_{(\mathfrak{l})}|\mathfrak{F}_{\mathfrak{l}+1}],$$

where $\mathbb{I}_A$ is an indicator function, $\mathbb{I}_A(x) = 1$ if $x \in A$ else $\mathbb{I}_A(x) = 0$. At least, such series of subsets must exist unless $b_{(\mathfrak{l})} = 0$, a.s., while it is still a question that how to find such series of subsets. Fortunately, the atoms in $\mathfrak{F}_{\mathfrak{l}}$ are not the elements in $\mathfrak{F}_{\mathfrak{l}+1}$ according to the discussion in the beginning of this section. So we use the symbol $\Omega_i^{\mathfrak{l}}$ instead, and rewritten the recurrence relation as bellow,

$$\mathbb{I}_{\Omega_i^{\mathfrak{l}}} b_{(\mathfrak{l}+1)}(\tau) = \mathbb{I}_{\Omega_i^{\mathfrak{l}}} b_{(\mathfrak{l})}(\tau) - \mathbb{E}[\mathbb{I}_{\Omega_i^{\mathfrak{l}}} b_{(\mathfrak{l})}|\mathfrak{F}_{\mathfrak{l}+1}], \tag{7}$$

and we name such a operation "unfolding" in the $\mathfrak{l}$-th layer as $\Omega_i^{\mathfrak{l}} \in \mathfrak{F}_{\mathfrak{l}}$. If the network "unfolding" in each layer, it is technically equivalent to denote that $\Omega_i^{\mathfrak{l}}$ takes the atoms of $\sigma(\cup_{l=0}^{\mathfrak{l}} \mathfrak{F}_l)$. The results of "unfolding" are displayed in Fig. 5 (c) and (d).

That is, for any nonlinear function which is uniformly differentiable and with bounded derivatives, it can be approximated by a linear function in a local area when the size of such a area tends to zero, so with the "unfolding" operation introduced in each layer the final loss will tend to loss of the linear function

TABLE I
TEST FUNCTIONS

Function	Range
$\frac{2}{D}\sum_{i=1}^{D} x_i + 0.1$	$[-1, 1]^D$
$\frac{2}{D}\sum_{i=1}^{D} \cos(5x_i + 0.1)$	$[-1, 1]^D$
$\frac{2}{D}\sum_{i=1}^{D} \exp(0.5x_i + 0.1)$	$[-1, 1]^D$

case. By now we can summarize the discussion in this section as the theorem bellow.

Theorem IV.3. *For any nonlinear target function which uniformly differentiable and with bounded derivatives, the DVSOM with "unfolding" in each layer has the estimation of loss. That is, for some positive number C_p,*

$$\log(\textbf{\textit{loss}}) \leq -p_0 \frac{\mathfrak{n}}{D} \log(N) + \log C_p. \tag{8}$$

Proof. For any $x_0 \in \mathbb{R}^D$ and a nonlinear uniformly differentiable function $f(x)$ in $\mathbb{R}^D$ space, there is a linear approximation $f(x) = k(x_0)(x - x_0) + b(x_0) + \mathfrak{o}(\|x - x_0\|)$ in the neighbourhood $\mathbf{U}(x_0; \delta)$, where $\mathfrak{o}(a)$ represent the higher order infinitesimal of a.

Meanwhile, this function is with bounded derivatives. It means that there exists a positive number C_k, so that $\sup_{x_0 \in \mathbb{R}^D} \|k(x_0)\| \leq C_k$, according to Remark IV.2, we get $\sup_{x_0 \in \mathbb{R}^D} \|p(k(x_0))\| \leq C_p$. By integrate the previous discussion in this section, Inequality (8) holds. □

Remark IV.4. *Rigorously, there is a small deviation in the estimation of C_p in the proof caused by $\mathfrak{o}(\|x - x_0\|)$. While, as discussed in the beginning of this section, the divided parts of input vectors space is $2^{\mathfrak{n}}$. It means the diameter of the x_0's neighbourhood is proportional to $2^{\frac{D}{\mathfrak{n}}}$. That is, the deviation caused by $\mathfrak{o}(\|x - x_0\|)$ is $\mathfrak{o}(2^{\frac{D}{\mathfrak{n}}})$ and it can be fixed by defining a constant $\tilde{C} > \mathfrak{o}(2^{\frac{D}{\mathfrak{n}}})$ and let $C_p \leftarrow C_p + \tilde{C}$. The correctness of the theorem is not affected.*

V. NUMERICAL EXPERIMENT

In this section, the convergence theorem is verified by a series of numerical experiments. At the beginning, we set $\alpha = 0.03$ and $\eta_{i,j} = \frac{1}{|i-j|+1}$, for $|i - j| \leq 1$ else $\eta_{i,j} = 0$. And the parameters $\mathcal{K}$ and $\mathcal{B}$ of batch normalization are updated by,

$$\begin{cases} \bar{X}_{(\mathfrak{l})} = \dfrac{1}{\Gamma}\displaystyle\sum_{\tau=1}^{\Gamma} X_{(\mathfrak{l})}(\tau), \\ \mathcal{B}_{\mathfrak{l}} \leftarrow 0.05\bar{X}_{(\mathfrak{l})} + 0.95\mathcal{B}_{\mathfrak{l}}, \\ \mathcal{K}_{\mathfrak{l}} \leftarrow 0.05\sqrt{\dfrac{1}{\Gamma}\displaystyle\sum_{\tau=1}^{\Gamma} (X_{(\mathfrak{l})}(\tau) - \bar{X}_{(\mathfrak{l})})^2} + 0.95\mathcal{K}_{\mathfrak{l}}. \end{cases}$$

Let the number of layers of DVSOM range from 1 to 5, that of neurons, denoted by N, in each layer range from 2 to 7 and the dimensions of input vectors, denoted by D, range from 1 to 5. And three test functions are selected, as shown in Table I, which represent the linear, the periodic and asymmetric cases. And for each test function, we randomly choose 5000 samples for training, as many as for testing. The testing result is listed in Figs. 6, 7 and 8. It can be seen that the logarithm of

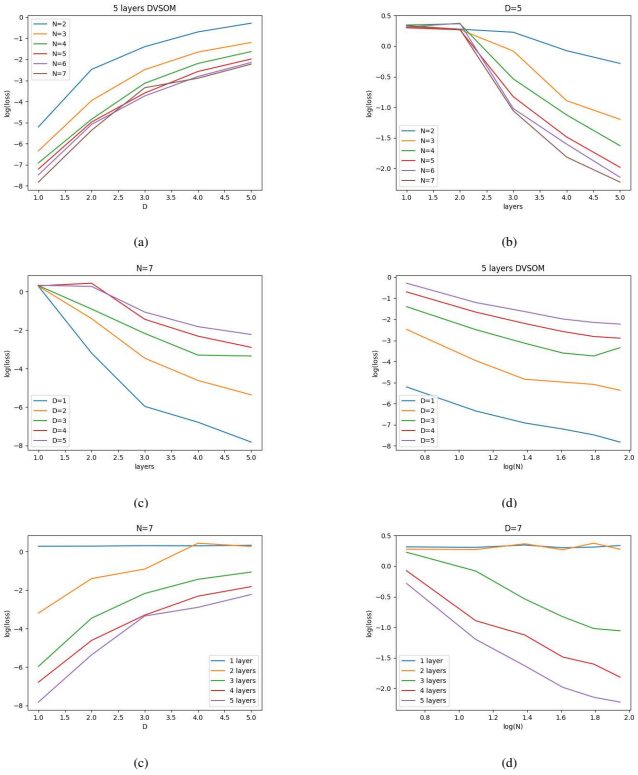

Fig. 6. The testing result for $\frac{2}{D}\sum_{i=1}^{D} x_i + 0.1$

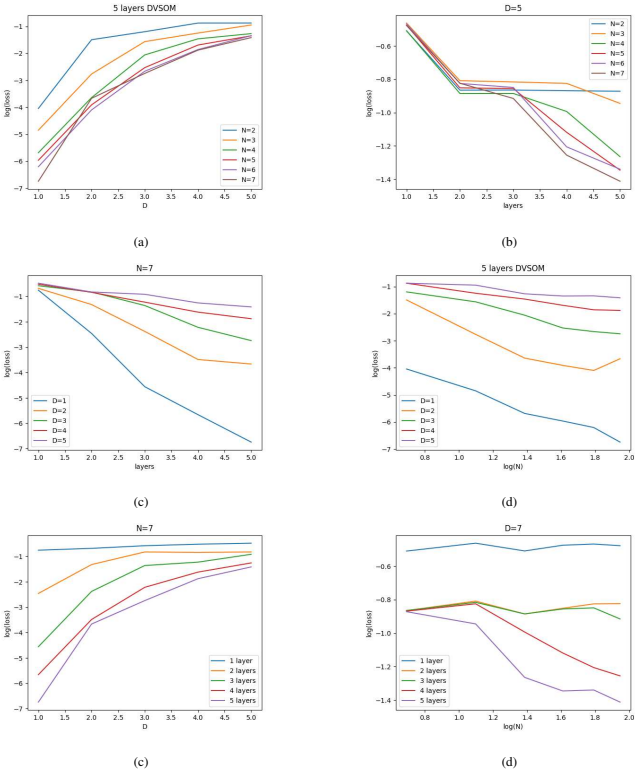

Fig. 7. The testing result for $\frac{2}{D}\sum_{i=1}^{D} \cos(5x_i + 0.1)$

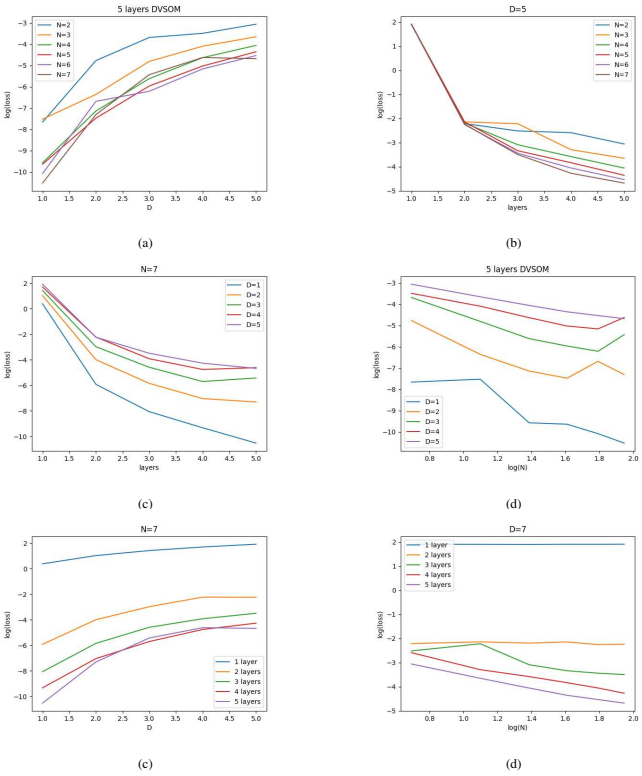

Fig. 8. The testing result for $\frac{2}{D}\sum_{i=1}^{D} \exp(0.5x_i + 0.1)$

loss is directly proportional to the number of network layers and the logarithm of the number of neurons in each layer, but inverse proportional to the dimension of input vectors. And when the number of network layers is low (1 2), seen Figs. 6(c)(d), 7(c)(d) and 8(c)(d), the expression ability of DVSOM is really limited, as we analyzed before.

VI. Conclusion

This paper has proposed a novel structure of deep learning and it training process is totally gradient-free. Through the innovation of SOM structure, we have introduced the Lethe into the original neuron to make the neuron equip with the ability of supervised learning, so that the ability can be extended to form VSOM layer. On this basis, differences between the input vectors and the best matching neuron and the residuals of Lethe have been taken as new inputs into the next VSOM layer with batch normalization on the differences. Meanwhile, "unfolding" has been added into each layer of the network to enhance the ability of spatial decomposition. On this basis, VSOM has gone deeper and finally formed DSOM. More importantly, the network convergence theory concerning with the structure' parameters has been proved and given an inequality about the relationship between depth, width, dimensions of space and the loss. Finally, numerical experiments has verified out convergence theory.

References

[1] Q. Le, J. Ngiam, A. Coates, A. Lahiri, B. Prochnow, and A. Ng, "On optimization methods for deep learning," vol. 2011, 2011, pp. 265–272.

[2] C. Cummins, P. Petoumenos, Z. Wang, and H. Leather, "End-to-end deep learning of optimization heuristics," in *2017 26th International Conference on Parallel Architectures and Compilation Techniques (PACT)*, 2017, pp. 219–232.

[3] H. Gupta, K. H. Jin, H. Q. Nguyen, M. T. McCann, and M. Unser, "Cnn-based projected gradient descent for consistent ct image reconstruction," *IEEE Transactions on Medical Imaging*, vol. 37, no. 6, pp. 1440–1453, 2018.

[4] T. Ichimura, K. Fujita, T. Yamaguchi, M. Hori, L. Wijerathne, and N. Ueda, "Fast multi-step optimization with deep learning for data-centric supercomputing," in *Proceedings of the 2020 4th International Conference on High Performance Compilation, Computing and Communications*, ser. HP3C 2020. New York, NY, USA: Association for Computing Machinery, 2020, p. 7–13. [Online]. Available: https://doi.org/10.1145/3407947.3407949

[5] T. Kohonen, "The self-organizing map," *Proceedings of the IEEE*, vol. 78, no. 9, pp. 1464–1480, 1990.

[6] R. Lasri, "Clustering and classification using a self-organizing map: The main flaw and the improvement perspectives," in *2016 SAI Computing Conference (SAI)*, 2016, pp. 1315–1318.

[7] J. Lampinen, "On clustering properties of hierarchical self-organizing maps," in *Artificial Neural Networks*. Amsterdam: North-Holland, 1992, pp. 1219 – 1222. [Online]. Available: http://www.sciencedirect.com/science/article/pii/B9780444894885500841

[8] A. Shimada and R. Taniguchi, "Gesture recognition using sparse code of hierarchical som," in *2008 19th International Conference on Pattern Recognition*, 2008, pp. 1–4.

[9] S. Furao and O. Hasegawa, "An incremental network for on-line unsupervised classification and topology learning," *Neural Networks*, vol. 19, no. 1, pp. 90–106, 2006.

[10] S. Furao, T. Ogura, and O. Hasegawa, "An enhanced self-organizing incremental neural network for online unsupervised learning." *Neural Networks the Official Journal of the International Neural Network Society*, vol. 20, no. 8, pp. 893–903, 2007.

[11] N. Liu, J. Wang, and Y. Gong, "Deep self-organizing map for visual classification," in *2015 International Joint Conference on Neural Networks (IJCNN)*, 2015, pp. 1–6.

[12] C. S. Wickramasinghe, K. Amarasinghe, and M. Manic, "Parallalizable deep self-organizing maps for image classification," in *2017 IEEE Symposium Series on Computational Intelligence (SSCI)*, 2017, pp. 1–7.

[13] K. He, X. Zhang, S. Ren, and J. Sun, "Deep residual learning for image recognition," in *2016 IEEE Conference on Computer Vision and Pattern Recognition (CVPR)*, 2016, pp. 770–778.

[14] M. W. Bara, N. B. Ahmad, M. M. Modu, and H. A. Ali, "Self-organizing map clustering method for the analysis of e-learning activities," in *2018 Majan International Conference (MIC)*, March 2018, pp. 1–5.

[15] J. Wesołowski, "Stochastic processes with linear conditional expectation and quadratic conditional variance," *Probability & Mathematical Statistics*, vol. 14, no. 1, pp. 33–44, 1993.

[16] R. Jarrow and A. Rudd, "Approximate option valuation for arbitrary stochastic processes," *Journal of Financial Economics*, vol. 10, no. 3, pp. 347–369, 2014.

[17] D. Xie, J. Xiong, and S. Pu, "All you need is beyond a good init: Exploring better solution for training extremely deep convolutional neural networks with orthonormality and modulation," in *2017 IEEE Conference on Computer Vision and Pattern Recognition (CVPR)*, 2017, pp. 5075–5084.

[18] Q. Yuan and N. Xiao, "Scaling-based weight normalization for deep neural networks," *IEEE Access*, vol. 7, pp. 7286–7295, 2019.

[19] W. Du and Y. Wang, "Stacked convolutional lstm models for prognosis of bearing performance degradation," in *2019 Prognostics and System Health Management Conference (PHM-Qingdao)*, 2019, pp. 1–6.

[20] Z.-Q. Zhao, H. Bian, D. Hu, W. Cheng, and H. Glotin, "Pedestrian detection based on Fast R-CNN and Batch Normalization," in *Intelligent Computing Theories and Application*, D.-S. Huang, V. Bevilacqua, P. Premaratne, and P. Gupta, Eds. Cham: Springer International Publishing, 2017, pp. 735–746.

[21] W. Yun, Z. Lu, K. Feng, X. Jiang, P. Wang, and L. Li, "Two efficient ak-based global reliability sensitivity methods by elaborative combination of bayes' theorem and the law of total expectation in the successive intervals without overlapping," *IEEE Transactions on Reliability*, vol. 69, no. 1, pp. 260–276, 2020.

[22] E. J. Mcshane, "Jensen's inequality," *Bulletin of the American Mathematical Society*, vol. 43, no. 8, pp. 521–527, 1937.